# Exploring the molecular basis for the metal-mediated assembly of alginate gels

Matthew B. Stewart[a,b*], Stephen R. Gray[a,b], Todor Vasiljevic[a,c] and John D. Orbell[a,b]

[a]Institute for Sustainability and Innovation (ISI), Victoria University, PO Box 14428, Melbourne, VIC 8001, Australia

[b]College of Engineering and Science, Victoria University, PO Box 14428, Melbourne, VIC 8001, Australia

[c]College of Health and Biomedicine, Victoria University, PO Box 14428, Melbourne, VIC 8001, Australia

***Corresponding Author –** Matthew B. Stewart, email: matthew.stewart@vu.edu.au, Telephone: +61 3 9919 7641, Mailing address: as above (a).

**Email addresses –** Matthew.Stewart@vu.edu.au; Stephen.Gray@vu.edu.au; Todor.Vasiljevic@vu.edu.au; John.Orbell@vu.edu.au.

## Abstract

The binding of sodium and calcium ions to single and multiple poly-G decamer strands has been modelled by conducting a series of molecular dynamics simulations. Implications for metal mediated inter-strand interactions and gel assembly have been explored by systematically introducing up to three strands into each of these simulations. A particular emphasis has been placed on revealing intrinsic binding modes by an unbiased initial positioning of the metal ions. The results have revealed binding modes that provide a rationale for the observed gelling of alginate by calcium rather than sodium ions. A number of junction zones involving calcium ions have been identified that result in chain aggregation. This includes a distinctive perpendicular motif that appears to be ubiquitous in previously reported AFM images of open 3-D alginate networks. The coordination geometries of the

metal ions have been characterized and the metal-mediated junctions between associated strands are described in detail.

***Keywords:*** Sodium alginate, Alginate gels, Molecular dynamics, Calcium coordination

## 1. Introduction

Alginate is the common term for a family of linear polyuronic acids isolated from brown algae (including several seaweed species) and some bacteria (Donati & Paoletti, 2009; Gorin & Spencer, 1966; Goven, Fyfe, & Jarman, 1981). Biologically, alginates are found in algal cell walls and intercellular mucilage, providing mechanical strength and flexibility - similar to the role played by cellulose and pectin in land-based plants (Donati & Paoletti, 2009). Alginates are also found in the protective cyst of *Azotobacter vilelandii* as well as in the biofilms produced by *Psuedomonas* and *Azotobacter* (Gorin & Spencer, 1966; Goven et al., 1981; Linker & Jones, 1966). Chemically, alginate chains consist of arrangements of β-D-mannuronic acid (M) and its C5 epimer, α-L-guluronic acid (G), bound *via* (1 → 4) glycosidic linkages, Fig. S1. Alginates are ionic at neutral pH, with a pKa around 3.8.

Isolated alginates (generally available as the $Na^+$ salt) are widely utilized throughout a number of industries, including as a common food additive and in a wide range of medical applications, from toothpastes to advanced wound dressings (BeMiller, 2009; Davis, Volesky, & Mucci, 2003; Donati & Paoletti, 2009; Langer & Tirrell, 2004). Such uses are generally related to their gelling and water-retaining properties. This sought-after gelling activity occurs when alginate chains aggregate in the presence of divalent cations (most commonly $Ca^{2+}$) that facilitate interchain interactions. Networks formed by such interchain aggregations may be visualized using techniques such as atomic force microscopy (Decho,

1999). We have relied upon the work of this author, in particular, in order to benchmark our MD results to experimental results. The areas where interchain interactions occur within these networks are commonly referred to as 'junction zones'. It has been shown previously that such junction zones may occur in G-rich areas of alginates and may display a preference for a free $Ca^{2+}$:G ratio of 1:4 (Grant, Morris, Rees, Smith, & Thom, 1973). An early attempt to define the specific nature of this interaction was the 'egg-box' model proposed by Grant and co-workers in 1973. This model proposed that $Ca^{2+}$ binding occurs between two parallel alginate chains, which assume a $2_1$ helical conformation. This model places the $Ca^{2+}$ ions in pockets, or depressions, formed naturally by the puckered structure imparted by the G-G α-glycosidic bond, Fig. S1. Questions have been raised in the literature as to whether this structure is viable experimentally (Braccini & Pérez, 2001). Several other subsequent models have also been suggested, including the 'shifted egg-box' model (Braccini & Pérez, 2001) and a modified shifted egg-box model, whereby only carboxylate oxygen atoms interact with the $Ca^{2+}$ ions (Plazinski, 2011). These previously published models of $Ca^{2+}$-poly-G interactions have assumed that all $Ca^{2+}$ interactions with G-rich sections involve parallel aggregation of the alginate chains and assume that there is only one mode of $Ca^{2+}$ interaction. As noted previously in the literature (Plazinski, 2011), the precise environment of the $Ca^{2+}$ ion in aggregated alginates is difficult to obtain using conventional analytical experimental techniques.

In this work, we have employed molecular dynamics methods to probe the binding of sodium and calcium ions to poly-G decamers in an aqueous environment - with a view to discerning preferred binding modes and their implications for interstrand interactions. Whilst the literature contains a number of previous theoretical studies which have attempted to provide insights into the specific binding site(s) of $Ca^{2+}$ with alginates, this earlier work has been

limited in scope and has tended to focus on confirming the widely accepted, if not entrenched, egg-box model (Braccini & Pérez, 2001; Li, Fang, Vreeker, & Appelqvist, 2007; Plazinski, 2011). The simulations carried out in the present work are designed to systematically characterize and compare the binding of charge-neutralising levels of $Na^{+}$ and $Ca^{2+}$ ions to the poly-G sequence (represented here by one, two and three decamer chains) in an aqueous environment, and to examine the nature of possible metal-mediated interactions leading to aggregation between alginate strands. A particular goal has been to reveal *intrinsic* interactions, either of an intermediate or an essentially consolidated nature. In this regard, these simulations differ from previously published investigations (Braccini, Grasso, & Pérez, 1999; Braccini & Pérez, 2001; DeRamos, Irwin, Nauss, & Stout, 1997; Plazinski, 2011) in that the initial placement of the metal ions is random in relation to the alginate chains, rather than at specific distances between two parallel or anti-parallel chains of the poly-G. This is to ensure that any structures formed are not a function of the initial starting geometry. Thus the aim is not to replicate the classical 'egg-box' model, which is usually assumed to result in the metal-mediated parallel association of strands, but rather to delineate possible variants and alternatives that might also promote non-parallel arrangements or motifs that could form the basis for open grid-like configurations. Such arrangements could represent precursor structures for the formation of 3-D gel networks and could be suggestive of assembly mechanisms.

## 2. Computational method

Simulations were carried out using a modified CHARMM all22 force field (MacKerell et al., 1998) and the NAMD 2.7 package (Phillips et al., 2005). Topology and parameter files for carbohydrates were edited to allow for the addition of the carboxylic acid groups. Atomic point charges were recalculated from density functional equilibrium geometry calculations, at

the B3LYP/6-31G(d) level of theory, on the G monomers and reapplied to the topology. Oligomers of the poly-G sequence, each 10 residues long and fully deprotonated, were constructed using the Visual Molecular Dynamics (VMD) program (Humphrey, Dalke, & Schulten, 1996) and optimised using MD in a TIP3P water box which measured 20 Å x 20 Å x 20 Å. These optimisations involved 2000 conjugate gradient minimization steps, followed by 2 ps of molecular dynamics simulation time under NVT conditions in a periodic box. The temperature and pressure was maintained using Langevin dynamics as implemented in NAMD. It must be noted that these initial optimisation simulations were not charge neutralised, as the effect of metal ions (including $Na^+$, which is the standard counter ion for alginates) was to be investigated. These optimised structures were used as starting geometries for the metal ion binding simulations.

The production simulations involved either one, two or (in the case of the $Ca^{2+}$ ion environments only) three oligomers. Where two oligomer chains were present, the identical sequences were placed parallel, approximately 6 Å apart; where three chains were used, and these were placed in a triangular array. TIP3P water was then added, again with 20 Å padding in all directions, as was the case for the optimisation simulations above. $Ca^{2+}$ ions were added randomly to the solvated system to neutralise the anionic charges of the oligomers. These ions were added *via* the Autoionize plugin in VMD with a minimum distance of 5 Å between the added ions and the solute or other ions. The ion placement was randomised so as to not bias the simulation towards a particular outcome. Each system was again subjected to 2000 conjugate gradient minimisation steps, followed by a simulated annealing procedure. This has been introduced in order to overcome the inherent energy barriers in these simulations whilst keeping the simulation time as short as possible. Achieving this by traditional optimization methods requires the initial state of the system, in terms of the positioning of the $Ca^{2+}$ ions, to

reflect the expected outcome of the simulation - an approach that has been adopted in all previous MD studies on metal/alginate systems, *vide supra.* Since a major objective of this work is to avoid such bias, this simulated annealing protocol has been successfully implemented in order to readily identify more intrinsic outcomes. Notably, this approach has been validated in this study by the observed consolidation of well-behaved metal coordination geometries that are in good agreement with experimental data (Dudev & Lim, 2004; Einspahr & Bugg, 1981; Katz, Glusker, Beebe, & Bock, 1996). A major advantage of this method is that highly informative structural outcomes are obtained in a relatively short simulation time of less than 1 ns. Specifically, the annealing procedure involved an initial increase in temperature to 650 K, with cooling of the system to 300 K in 50 K increments at 100 ps intervals, giving a final runtime of 0.8 ns. An NVT-ensemble and periodic boundary conditions were utilised for these annealing simulations with the temperature controlled *via* rescaling of all velocities every 2 ps. The equations of motion were integrated at 1 fs timesteps. Short-range nonbonded interactions were calculated at a 1 ps timestep with a Van der Waals switching distance of 10 Å and overall nonbonded cutoff at 12 Å with long-range interactions integrated every 2 ps using the r-RESPA integrator. The Particle mesh Ewald (PME) method was used to describe the full-system periodic electrostatics. The short-range pairlist was updated every 10 ps for atoms within 14 Å. The simulation trajectory was written every 500 fs in order to provide good quality data with respect to interactions. All single chain simulation trajectories were analysed *via* calculation of the radial distribution functions for specific oxygen-metal ion interactions, utilising the g(r) GUI plugin of VMD (Humphrey et al., 1996).

## 3. Convention

The numbering scheme for the G monomer with respect to the oxygen atoms, and the convention for referring to these atoms at different locations in the chain, is given in Fig. 1.

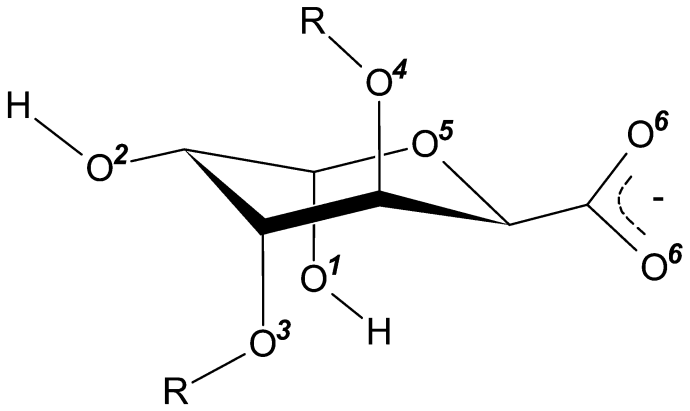


**Fig. 1.** The G alginate monomer, α-L-guluronate, showing the numbering scheme with respect to the oxygen atoms. Note: Atoms referred to in the text that are in an adjacent monomer are marked with a dash; a double dash refers to atoms located two monomers away; an asterisk indicates that an atom is on a second chain; O6 refers to the oxygens of a delocalized carboxylate anion.

Simulations involving a single alginate decamer are denoted by 1 x poly-G, those involving two such chains are denoted by 2 x poly-G and those involving three such chains are denoted by 3 x poly-G.

## 4. Results and discussion

The metal ion oligomer interactions observed in this study are generally formed rapidly - with $Ca^{2+}$ interactions consolidating sooner within the simulations than $Na^{+}$. Notably, chains were observed to aggregate only in the presence of $Ca^{2+}$ ions. This is consistent with experimental observations regarding the solubility of alginates in the presence of monovalent cations and hydrogel formation in the presence of divalent or multivalent cations (Donati & Paoletti, 2009). It is acknowledged that this study relates to decamers only and may not directly reveal the influence of chain length on the longer term aggregation dynamics (Kohn, 1975). However, this work has been designed to specifically investigate the *initial* stages of aggregation, the motifs of which may then form the basis for subsequent cooperative

aggregation. The detailed interactions of $Ca^{2+}$ and $Na^{+}$ with the poly-G decamer are described as follows:

*4.1. 1 x Poly-G*

When a single poly-G chain, in the presence of water and $Ca^{2+}$ ions is simulated, two distinct binding interactions are identified. The most prevalent interaction, which involves four of the five $Ca^{2+}$ ions available in this simulation, involves direct binding to carboxylate groups. These $Ca^{2+}$ ions are each coordinated to one carboxylate oxygen and between five and six water molecules. A consistent feature of these interactions is the hydrogen bonding that is observed to occur between one of the coordinated water molecules and the O3 atom of the neighbouring guluronate residue, Fig. S2. Such 'water bridging' would be expected to stabilise such interactions. The other identified interaction is similar, although not exactly identical to, the classical egg-box model, Fig. 2. This interaction involves four coordinating oxygen atoms from the poly-G, reflecting the egg-box model, and four coordinated water molecules. Whereas the classical egg-box model postulates five coordinating atoms per alginate chain, specifically O`6, O`5, O2, O3 and O1, the interaction identified in this study forms through direct coordination with the O`6, O2, O3 and O1 atoms only - with one of the coordinated water molecules forming a water bridge to the O`5 atom. For this binding mode, Fig. 3a plots the distance of the coordinating oxygen atoms from the $Ca^{2+}$ ion as a function of the simulation time. It can be seen from Fig. 3a that the interaction distances appear to be relatively stable from approximately 0.4 ns onwards, which corresponds to an annealing temperature of simulation of 450 K. Only three oxygen atoms of the guluronate (O`6, O2 and O3) can be considered to be tightly bound to the $Ca^{2+}$ - with average bound distances of 2.16 ± 0.7 Å, 2.45 ± 0.16 Å, and 2.42 ± 0.17 Å, respectively.

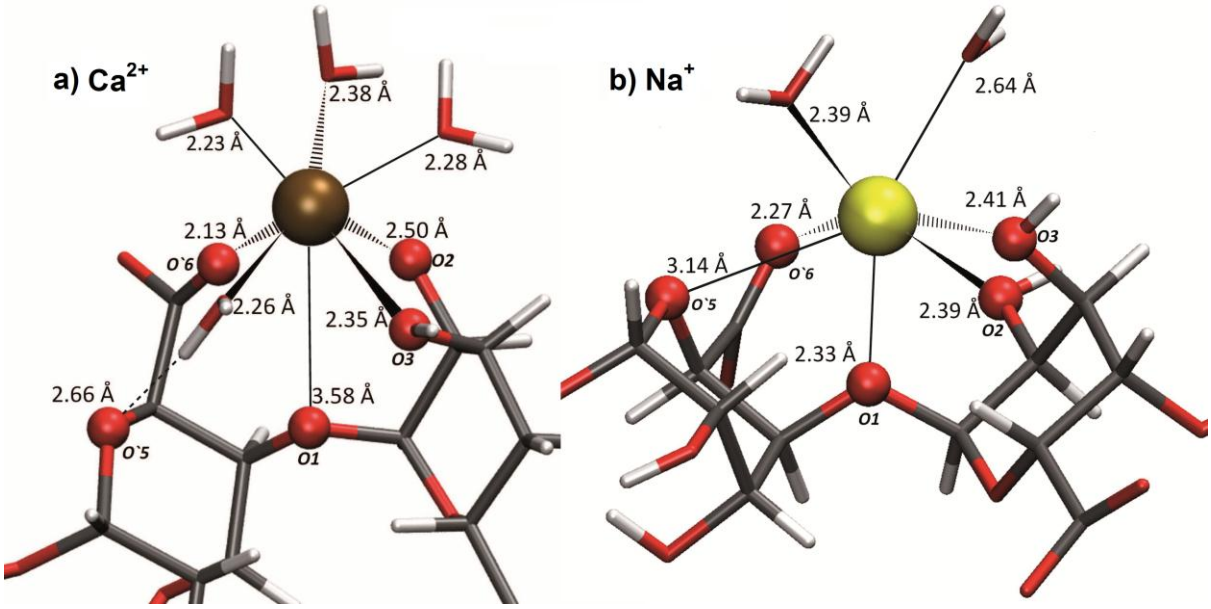


**Fig. 2. a)** The egg-box binding site for $Ca^{2+}$ (brown sphere); note the water bridge to the O'5 atom. **b)** The egg-box binding site for $Na^{+}$ (yellow sphere). In **a)** and **b)** oxygen atoms on the poly-G chain are shown as red spheres; coordinated water molecules are shown as stick formulae.

The O1 atom exhibits only a weak interaction with the $Ca^{2+}$ - at an average distance of 3.23 ± 0.5 Å and the O`5 atom is not considered to be close enough to the $Ca^{2+}$ ion to exert a direct influence - with an average distance of 4.13 ± 0.6 Å. This coordination geometry does not strictly agree with the classical egg-box model, which proposes that all five oxygen atoms described here interact directly with the $Ca^{2+}$ ion (Grant et al., 1973). Rather, it is in closer agreement with the revisited egg-box model of Braccini and Pérez, where interactions with O2 and O3 are also identified, and which does not attribute a role to the O`5 oxygen atom (Braccini & Pérez, 2001). Thus the interaction observed here can be regarded as a hybrid of these two models. Whilst only four oxygen atoms are directly interacting with the $Ca^{2+}$ ions, the O`5 atom interacts with the $Ca^{2+}$ ion via a coordinated water molecule (water bridging), Fig. 2a.

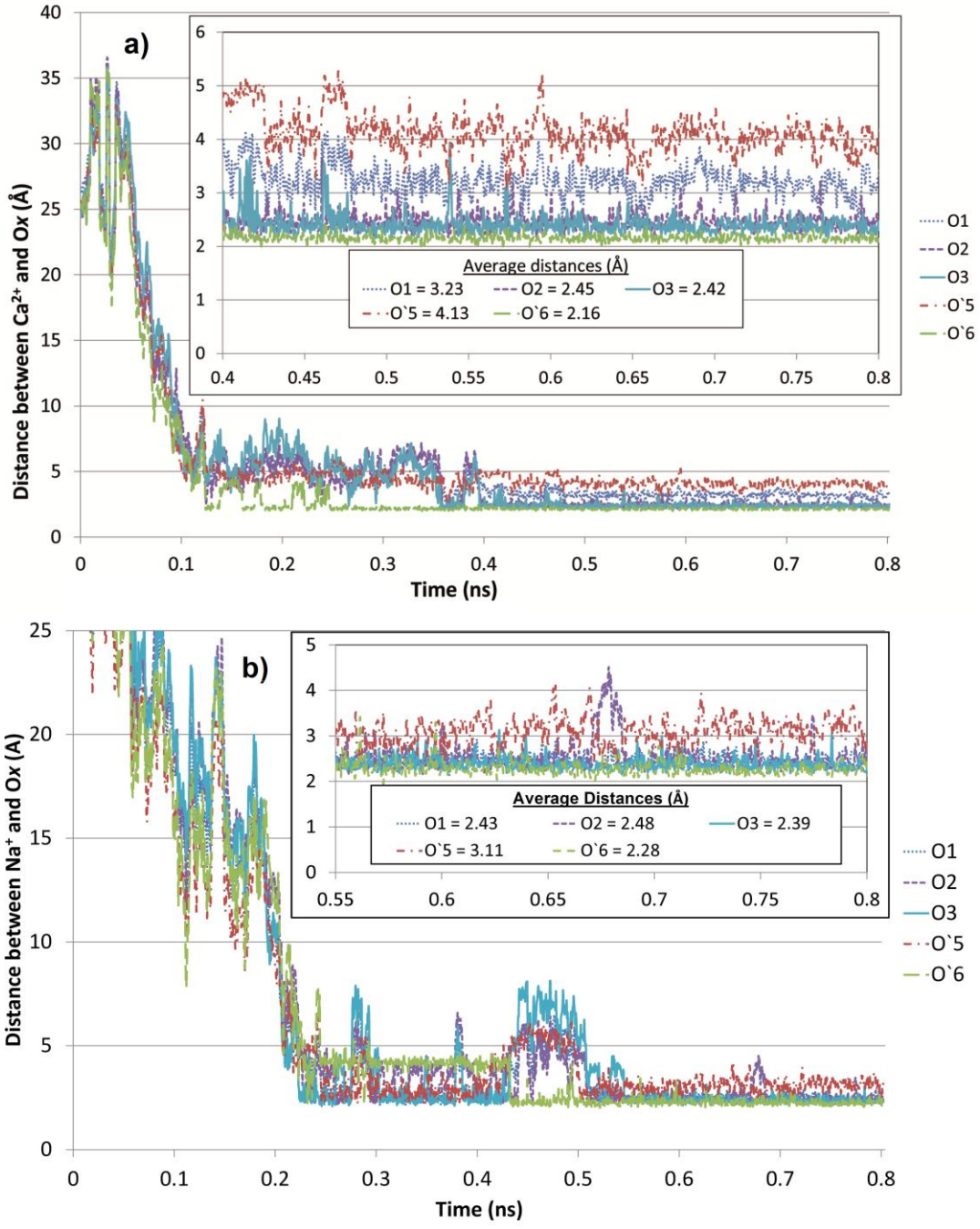


**Fig. 3. a)** The distances between the $Ca^{2+}$ ion and the bonding oxygen atoms in the variant of the egg-box structure as identified in the single poly-G chain simulation. Note the apparent stability in these distances from approximately 0.4 ns - suggesting a consolidation of the interaction. **b)** Distances from the coordinating $Na^{+}$ ion with the five interacting oxygen atoms of the single poly-G chain at the binding site between residues 3 and 4 of the decamer. The inset plots are magnifications of the last 0.4 and 0.25 ns respectively.

Fig. 4 shows the corresponding radial pair distribution function, g(r), for $Ca^{2+}$ versus the five coordinating alginate oxygen atoms.

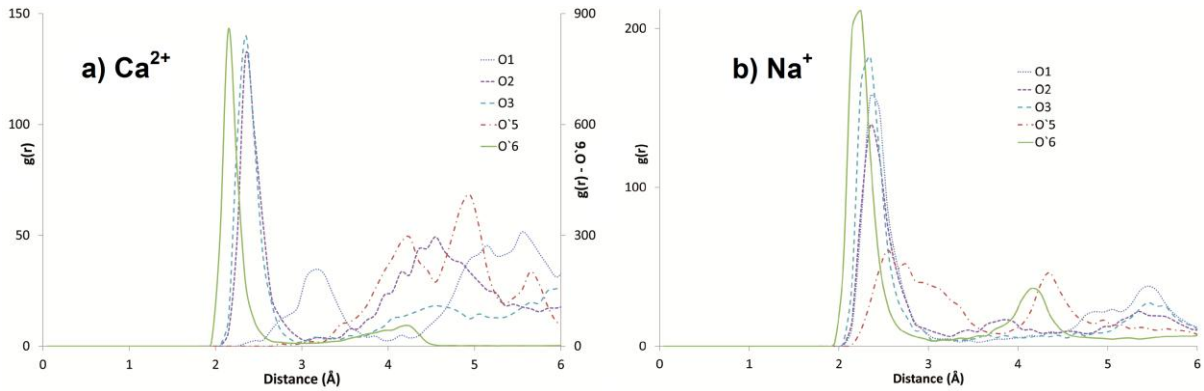


**Fig. 4.** Comparative radial distribution functions, g(r), for **a)** $Ca^{2+}$ and **b)** $Na^{+}$ against each of the oxygen atoms of interest in the poly-G sequence. In **a)**, the g(r) function values for the O`6 atom are plotted on the secondary axis.

This plot clearly shows that $Ca^{2+}$ displays a high preference (i.e. interaction probability – g(r)-O'6 is plotted separately on the right hand vertical axis) for binding to the negatively charged carboxylate moiety, O'6; at about 2.13 Å. O2 and O3 also bind directly to $Ca^{2+}$ at about 2.5 Å, which is consistent with the data presented in Fig. 3. The O`5 atom shows no direct interaction with the $Ca^{2+}$ in the g(r) plot (i.e. less than approximately 3 Å). However it does show some interaction with $Ca^{2+}$ occurring at distances between 4.3 and 5 Å, via a water-bridging interaction.

When this same single chain system is simulated in the presence of $Na^{+}$ ions, there is a markedly different interaction profile compared to $Ca^{2+}$. The dominant interaction in this simulation is the $Na^{+}$ equivalent to the classical egg-box structure as previously postulated for $Ca^{2+}$, Fig. 2b. To the best of our knowledge, this has not been previously characterized in the literature.

In this simulation, two such binding sites are found – that have $Na^+$ directly coordinated to the O`6, O`5, O2, O3 and O1 atoms (as required by the classical $Ca^{2+}$-based egg-box model) whilst the third binding site does not fully coordinate the O`5 atom, Fig. 2b. However, as this occurs in a terminal residue, there is expected to be additional conformational flexibility at this site (i.e. an 'end effect'). There are also two identified occurrences of water-bridged $Na^+$-carboxylate interactions analogous to those identified for $Ca^{2+}$, Fig. S2; with the other five $Na^+$ ions present in the simulation not interacting with the chain. The relative proportions of these interactions varied over the simulation time, as the interactions between the $Na^+$ and poly-G chain were not as stable as for the $Ca^{2+}$ simulation, with a higher degree of reversibility of the binding modes. This is evident in Fig. 3b that plots the $Na^+$-oxygen distances for one of the $Na^+$ binding sites identified in this simulation. When compared to Fig. 3b, the radial pair distribution function, g(r), for $Na^+$, Fig. 4b, highlights the preference of this ion for the full (classical) egg-box binding with the atoms of the coordination sphere, including the carboxylate, showing roughly equivalent probabilities of interaction.

It is of interest to compare the egg-box structures of $Ca^{2+}$ and $Na^+$ as depicted in Fig. 2 a) and b) respectively. The $Ca^{2+}$ ion may be seen to sit noticeably higher in the binding pocket than the $Na^+$. This is reflected in the selected relative distances and coordination angles provided in Table 1 and, at first glance, might be considered to be counterintuitive - given that both ions have very similar ionic radii and $Ca^{2+}$ has double the charge of $Na^+$. However, it should be noted that, relative to $Na^+$, the binding of the $Ca^{2+}$ is dominated by an interaction with the negatively charged carboxylate donor atom, O'6, (due to its +2 charge). This is reflected in the relative radial distribution functions for the bound $Ca^{2+}$ and $Na^+$ ions, Figs. 4a and b, respectively. It is clear from these analyses that the $Ca^{2+}$ is approximately six times more likely to be bound to the O'6 that to the other atoms within the coordination sphere. This is not the case for $Na^+$, where there is a more symmetric binding arrangement within the

coordination sphere, Fig. 2. This has the effect of raising the $Ca^{2+}$ ion within the pocket since the carboxylate moiety is orientated vertically. This effect is also enhanced by the presence of a water bridge from the $Ca^{2+}$ to the O'5 atom rather than a direct interaction. This seemingly subtle phenomenon suggests an explanation, at the molecular level, as to why $Na^{+}$, unlike $Ca^{2+}$, does not take part in metal mediated chain aggregation, since, unlike $Ca^{2+}$, it sits too low into the binding pocket to be accessible to another strand. This is coupled with the fact that $Na^{+}$, due to its more even affinity with all the oxygens in the coordination environment, including the carboxylate, Fig. 2, is more likely to associate with poly-G via such binding pockets than to form inter-strand carboxylate bridges (as is observed for $Ca^{2+}$ in this study).

**Table 1.** Comparison of the average angles and distances involved in the calcium and sodium egg-box structures.

| **Angle** | **M = Sodium** | **M = Calcium** | **Δ (Ca – Na)** |
|---|---|---|---|
| **O2-M-O'6** | 151.00° | 124.12° | -26.88° |
| **O1-M-O'6** | 82.04° | 61.82° | -20.22° |
| **O1-M-O2** | 70.11° | 57.93° | -12.18° |
| **O1-M-O3** | 76.21° | 63.43° | -12.78° |
| **Distance** | | | |
| **M-O1** | 2.43 Å | 3.23Å | 0.8 Å |
| **M-O2** | 2.48 Å | 2.45 Å | -0.03 Å |
| **M-O3** | 2.39 Å | 2.42 Å | -0.03 Å |
| **M-O'5** | 3.11 Å | 4.13 Å | 1.02 Å |
| **M-O'6** | 2.28 Å | 2.16 Å | -0.12 Å |

*4.2 2 x Poly-G*

When this system is modelled with $Na^{+}$ ions in the surrounding environment, several more transient instances of the same egg-box binding modality identified previously, Fig. 2, are observed in both of the individual chains. A number of fleeting interactions with single carboxylate groups are also observed. At no point during the simulation did the two chains show signs of $Na^{+}$-mediated aggregation, which is consistent with experimental observations regarding the solubility of alginate in the presence of low concentrations of monovalent cations (Donati & Paoletti, 2009).

When a simulation involving two poly-G chains in the presence of $Ca^{2+}$ is carried out, an interesting phenomenon is observed. The two poly-G chains are seen to aggregate almost perpendicular to each other, Fig. 5, with the junction zone being mediated by no less than three calcium ions.

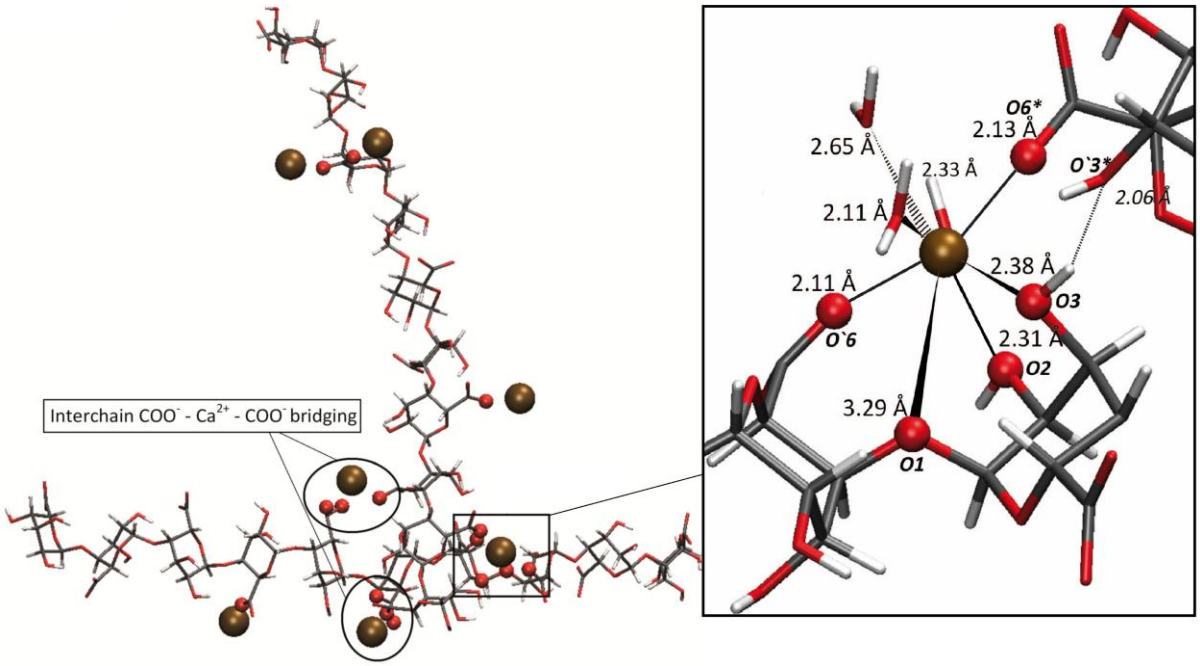


**Fig. 5.** Two poly-G chains aggregating in a perpendicular motif, *via* three bridging $Ca^{2+}$ ions (brown spheres). Inset highlights the details of the egg-box component of this junction zone. The two buttressing $Ca^{2+}$ interchain carboxylate bridges are also shown, as is the interchain hydrogen bond. Oxygen atoms that are directly interacting with a calcium ion are rendered as small red spheres.

This novel arrangement incorporates an egg-box type $Ca^{2+}$ binding modality (highlighted) which is very similar to the interaction observed with $Ca^{2+}$ and the single poly-G chain in Section 4.1, Fig. 2a. This 'pocket' interaction is reinforced by two interchain carboxylate-$Ca^{2+}$-carboxylate bridges adjacent to the egg-box interaction and by an interchain hydrogen bond, Fig 5.

More specifically, a $Ca^{2+}$ ion is embedded into a pocket between two G units and coordinates to four oxygen atoms (O1, O2, O3 and O`6) on one of the chains. The second poly-G chain then interacts with this embedded $Ca^{2+}$ ion *via* a carboxylate oxygen, O6*, with three water

molecules completing the coordination sphere. The chain aggregation is further enhanced by an interchain hydrogen bond between the hydroxyl hydrogen on the coordinated O3 oxygen (of the first chain) and the O3 atom one residue removed from the binding site of the second chain, and by the aforementioned two $Ca^{2+}$ ions that form concomitant interchain bridges between carboxyl groups, Fig. 5. This binding junction, involving three $Ca^{2+}$ ions in two different binding modes and defining two poly-G sequences in an approximate perpendicular arrangement, is new to the literature. In terms of the rigidity (stability) of the motif, it should be pointed out that the ratio of residues to calcium ions is 2:1, the same as in the parallel "egg-box" junction model (Grant et al., 1973). Three $Ca^{2+}$ ions at junctions of this type would be entirely consistent with the observed stability of such gels. This motif appears to be quite stable, forming and subsisting for the final 0.35 ns of simulation time, albeit with a slight fluctuation in the intermolecular hydrogen bond, Fig. 6.

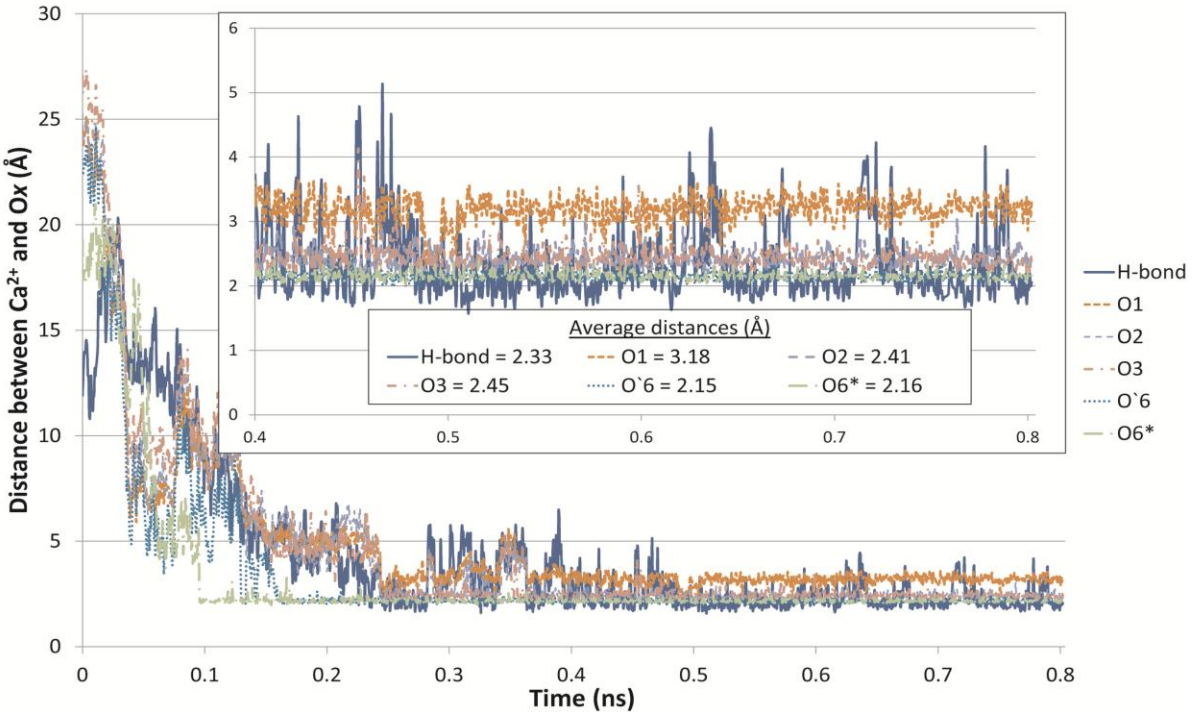


**Fig. 6.** A plot of the oxygen-$Ca^{2+}$ distances of the atoms involved in the egg-box binding site depicted in Fig. 5. Also shown is the interchain hydrogen bond that is formed between a coordinating water molecule and the O`3* atom.

The distinctive perpendicular motif described above, is a significant finding since it appears to be ubiquitous in AFM images of open 3-D alginate networks (Decho, 1999). Furthermore, due to the fact that this orientation involves non-terminal G resides, it might be expected that this could occur regardless of the length of the alginate chain. This observation does not imply that G-rich regions of alginate cannot form parallel associations or that they always aggregate perpendicularly; however these results do demonstrate that, under certain conditions, cross-linking type interactions such as this *may* occur between G regions of alginates. It is worth emphasizing that this aggregation is mediated by no less than three $Ca^{2+}$ ions, one of which utilizes a geometry similar to the shifted egg-box model (Braccini & Pérez, 2001). These results support the notion that it is possible for G-rich regions to form not only strong parallel associations but also strong *perpendicular* interchain associations. Furthermore, the two supporting interchain carboxylate-$Ca^{2+}$ bridges concomitant to the embedded $Ca^{2+}$, plus the interchain hydrogen bond would be expected to provide a degree of rigidity to this perpendicular arrangement by decreasing the range of possible movements of the poly-G chains.

*4.3 3x Poly-G*

When a third poly-G decamer is added, in the presence of neutralizing $Ca^{2+}$ ions, the resultant aggregation is consistent with previously published theoretical models (Braccini & Pérez, 2001; Grant et al., 1973; Plazinski, 2011). Here, the three chains self-organize approximately parallel, with two of the chains associating more strongly than the third. Thus the two closer chains share five metal-mediated interchain interactions of the carboxylate bridging type - although two sites also invoke binding from a nearby O3 atom, Fig. 7. The third chain associates at only one metal-mediated interaction site, which is *via* a carboxylate bridge. As

364 further evidence that the $Ca^{2+}$ mediated binding of the poly-G chains occurs *via* a variety of
365 mechanisms, rather than by the egg-box model exclusively, this simulation shows the $Ca^{2+}$
366 ions to interact almost exclusively *via* consolidated carboxylate bridging interactions, similar
367 to the model previously proposed by Plazinsky in 2011. Whilst one egg-box site is identified,
368 this site is disrupted due to steric influences from the second chain attempting to interact
369 through a carboxylate group. Although not as conducive to the formation of open 3-D
370 networks as the previously described perpendicular motif, a parallel aggregation of strands
371 (thickening) with associated branching is also suggested by available AFM images of such
372 networks (Decho, 1999).

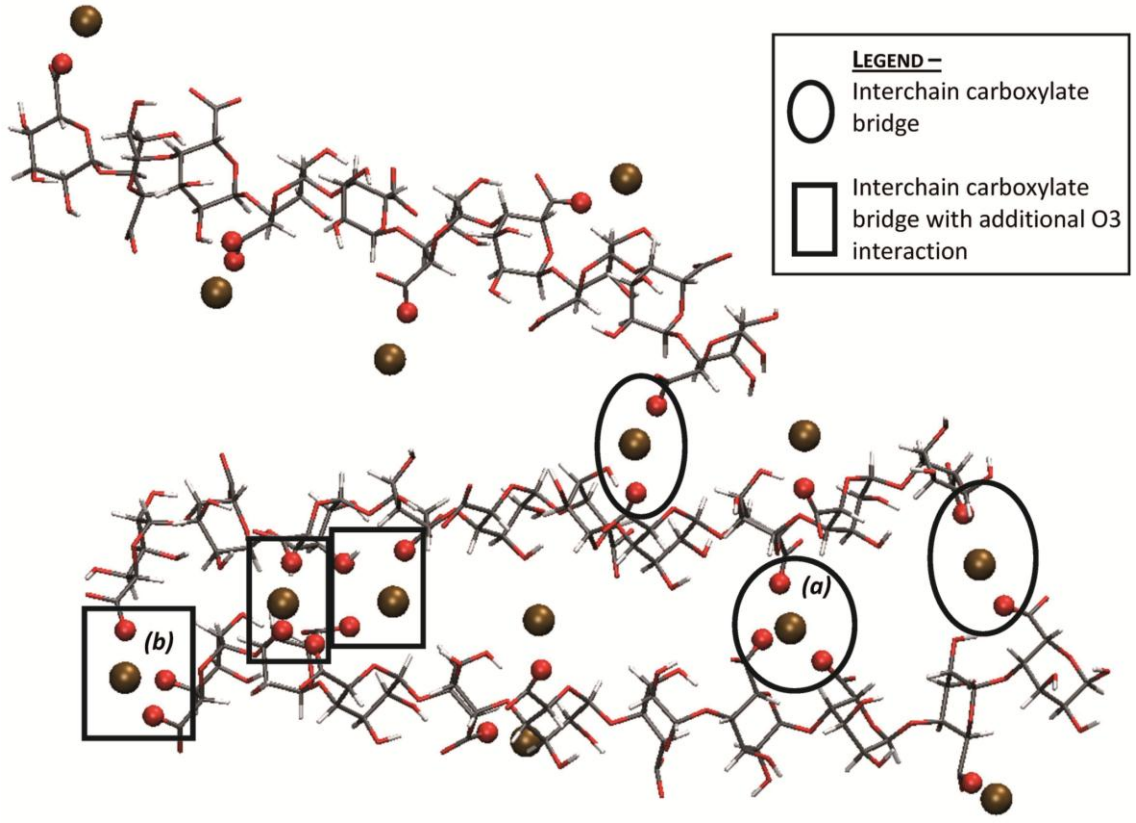


373
374
375
376 **Fig. 7.** Three poly-G chains aggregating in an approximately parallel arrangement in the
377 presence of $Ca^{2+}$ ions (shown in brown). Oxygen atoms directly interacting with the $Ca^{2+}$ ions
378 are shown as red spheres. The interchain interaction labelled **(a)** is a carboxylate bridge with
379 three carboxylate oxygens contributing, and **(b)** involves an O4 atom rather than an O3,
380 however this is due to an end-chain effect.
381

To what extent these structures represent intermediate or conserved motifs in the assembly mechanism would obviously require more enquiry. However, it may be surmised that, with further simulation time, the 3x poly-G parallel arrangement, in particular, could relax into an egg-box coordination pattern. Such relaxations, from metal-mediated carboxylate bridging to consolidated egg-box-type binding sites, might suggest a molecular basis for the experimentally observed syneresis identified in alginate hydrogels (Donati et al., 2005; Donati & Paoletti, 2009).

## 5. Conclusions

As described above, the MD method and simulations presented here have resulted in the characterisation of a variety of intrinsic binding modes for the interaction of sodium and calcium ions with single and multiple poly-G decamers that have implications for chain aggregation. All the coordination geometries, in terms of coordination numbers, bond lengths and angles, are well-behaved and as expected for the ions studied, which is a strong validation for the incorporation of the simulated annealing protocol. A slight variant on the classical egg-box binding mode was revealed with respect to $Ca^{2+}$ binding and an analogous (though not identical) mode for $Na^{+}$ has been characterized for the first time. A detailed comparison of the coordination spheres of these two ions provides a compelling structural rationale for the inability of $Na^{+}$ compared to $Ca^{2+}$ to induce chain aggregation - as is observed both experimentally and via simulation (this study). Several potential motifs have been uncovered that are consistent with previously reported molecular-scale imaging of an alginate gel network formed in the presence of such ions. Particularly noteworthy is the discovery of a stable perpendicular motif, mediated by three $Ca^{2+}$ ions, that appears to be ubiquitous in such images and that could provide an important structural basis for the assembly of open 3-D networks. Overall, direct interactions of both ions with single carboxylate moieties are common and water-bridging interactions from the metal to oxygen

atoms are also observed, as is inter-chain hydrogen bonding. This study provides significant insights into the intrinsic interactions of sodium and calcium ions with poly-G and how such interactions might underpin the assembly of open 3-D gels.

**Acknowledgements**

The authors would like to acknowledge Victoria University for providing a Postdoctoral Fellowship to MBS and the Victorian Partnership for Advanced Computing (VPAC) for providing computational time and expertise.

## References

BeMiller, J. N. (2009). One hundred years of commercial food carbohydrates in the United States. *Journal of Agricultural and Food Chemistry, 57*(18), 8125-8129.

Braccini, I., Grasso, R. P., & Pérez, S. (1999). Conformational and configurational features of acidic polysaccharides and their interactions with calicum ions: a molecular modeling investigation. *Carbohydrate Research, 317*, 119-130.

Braccini, I., & Pérez, S. (2001). Molecular basis of $Ca^{2+}$-induced gelation in alginates and pectins: The egg-box model revisited. *Biomacromolecules, 2*, 1089-1096.

Davis, T. A., Volesky, B., & Mucci, A. (2003). A review fo the biochemistry of heavy metal biosorption by brown algae. *Water Research, 37*(18), 4311-4330.

Decho, A. W. (1999). *Carbohydrate Research, 315*, 330.

DeRamos, C. M., Irwin, A. E., Nauss, J. L., & Stout, B. E. (1997). $^{13}C$ NMR and molecular modeling studies of alginic acid binding with alkaline earth and lanthanide metal ions. *Inorganica Chimica Acta, 256*, 69-75.

Donati, I., Holtan, S., Mørch, Y. A., Borgogna, M., Dentini, M., & Skjåk-Bræk, G. (2005). New hypothesis on the role of alternating sequences in calium-alginate gels. *Biomacromolecules, 6*, 1031-1040.

Donati, I., & Paoletti, S. (2009). Material Properties of Alginates. In B. H. A. Rehm (Ed.), *Alginates: Biology and Applications*: Springer Berlin Heidelberg.

Dudev, T., & Lim, C. (2004). Monodentate versus bidentate carboxylate binding in magnesium and calicum proteins: What are the basic principles? *Journal of Physical Chemistry B, 108*, 4546-4557.

Einspahr, H., & Bugg, C. E. (1981). The geometry of calcium-carboxylate interactions in crystalline complexes. *Acta Crystallographica, B37*, 1044-1052.

Gorin, P. A. J., & Spencer, J. F. T. (1966). Exocellular alginic acid from *Azotobacter Vinelandii*. *Canadian Journal of Chemistry, 44*, 993-998.

Goven, J. R., Fyfe, J. A., & Jarman, T. R. (1981). Isolation of alginate-producing mutants of *Pseudomonas fluorescens*, *Pseudomonas putida* and *Psuedomonas mendocina*. *Journal of General Microbiology, 125*, 217-220.

Grant, G. T., Morris, E. R., Rees, D. A., Smith, P. J. C., & Thom, D. (1973). Biological interactions between polysaccharides and divalent cations: The egg-box model. *FEBS Letters, 32*(1), 195-198.

Humphrey, W., Dalke, A., & Schulten, K. (1996). VMD - Visual Molecular Dynamics. *Journal of Molecular Graphics, 14*, 33-38.

Katz, A. K., Glusker, J. P., Beebe, S. A., & Bock, C. W. (1996). Calcium ion coordination: A comparison with that of beryllium, magnesium and zinc. *Journal of the American Chemical Society, 118*, 5752-5763.

Kohn, R. (1975). Ion binding on polyuronates - alginate and pectin. *Pure and Applied Chemistry, 42*, 371-397.

Langer, R., & Tirrell, D. A. (2004). Designing materials for biology and medicine. *Nature, 428*, 487-492.

Li, L., Fang, Y., Vreeker, R., & Appelqvist, I. (2007). Reexamining the Egg-Box Model in Calcium - Alginate Gels with X-ray Diffraction. *Biomacromolecules, 8*, 464-468.

Linker, A. J., & Jones, R. S. (1966). A new polysaccharide resembling alginic acid isolated from *Pseudomonads*. *Journal of Biological Chemistry, 241*, 3845-3851.

MacKerell, A. D., Bashford, D., Bellott, Dunbrack, R. L., Evanseck, J. D., Field, M. J., . . . Karplus, M. (1998). All-Atom Empirical Potential for Molecular Modeling and Dynamics Studies of Proteins. *The Journal of Physical Chemistry B, 102*(18), 3586-3616. doi: 10.1021/jp973084f

Phillips, J. C., Braun, R., Wang, W., Gumbart, J., Tajkhorshid, E., Villa, E., . . . Schulten, K. (2005). Scalable molecular dynamics with NAMD. *Journal of Computational Chemistry, 26*, 1781-1802.

Plazinski, W. (2011). Molecular basis of calcium binding by polyguluronate chains. Revising the egg-box model. *Journal of Computational Chemistry, 32*(14), 2988-2995.